

Proceedings Classification: Chemistry

Key Terms: nonlinear optics, computation, electric field, cyanine, polyene.

AN INVESTIGATION OF THE INTERRELATIONSHIPS BETWEEN  
LINEAR AND NONLINEAR POLARIZABILITIES AND BOND  
LENGTH ALTERNATION IN CONJUGATED ORGANIC MOLECULES

Christopher B. Gorman<sup>†</sup> and Seth R. Marder<sup>†,‡</sup>

<sup>†</sup>Jet Propulsion Laboratory, California Institute of Technology,  
4800 Oak Grove Drive, Pasadena, CA 91109, USA

<sup>‡</sup>The Beckman Institute, California Institute of Technology,  
Pasadena, CA, 91125, USA

**Abstract**

A computational method was devised to explore the relationship between charge separation, geometry, molecular dipole moment ( $\mu$ ), polarizability ( $\alpha$ ), and hyperpolarizabilities ( $\beta$ ,  $\gamma$ ) in conjugated organic molecules. It is shown that bond length alternation (the average difference in length between single and double bonds in the molecule) is a key structurally observable parameter that can be correlated with hyperpolarizabilities and is thus relevant to the optimization of molecules and materials. Using the method, the relationship between bond length alternation,  $\mu$ ,  $\alpha$ ,  $\beta$ , and  $\gamma$  for linear conjugated molecules is illustrated, and those molecules with maximized  $\alpha$ ,  $\beta$ , and  $\gamma$  are described.

## Introduction

Nonlinear optical (NLO) effects result from the polarization induced in a material by an intense electric field,  $\mathbf{E}$ . In organic materials, these effects can ultimately be traced back to the **orientationally** averaged sum of the induced polarizations of individual molecules. The induced polarization in a molecule,  $\mu_i$ , can be approximated by an expansion:

$$\mu_i = \alpha_{ij}E_j + \frac{\beta_{ijk}}{2}E_jE_k + \frac{\gamma_{ijkl}}{6}E_jE_kE_l + \dots \quad (1)$$

The first coefficient,  $\alpha$  is the linear polarizability and is related to the first derivative of the dipole moment with respect to  $\mathbf{E}$ . The higher order terms  $\beta$  and  $\gamma$  are referred to as the first and second hyperpolarizabilities. The polarization associated with these higher order coefficients are responsible for second- and third-order NLO effects. In this paper we discuss a computational method that predicts structural features of molecules that have maximized  $\alpha$ ,  $\beta$ , and  $\gamma$  for a given molecular length. Throughout, we will emphasize what we believe to be a key, experimentally accessible structural parameter, *bond length alternation* and illustrate the correlation between it and nonlinear optical response.

Prototypical organic chromophores for second-order nonlinear optics contain a **polarizable**  $n$ -electron system and donor and acceptor groups to create an asymmetric polarizability in the molecule. It has been recently hypothesized that there is an optimal combination of donor/acceptor strengths that will maximize  $\beta$  (1). This analysis has been based upon a two-state

model for  $\beta$  derived from static perturbation theory (2, 3) in which the dominant contribution to  $\beta$  arises from the ground state and a charge-transfer excited state. In this two-state model:

$$\beta \propto (\mu_{ee} - \mu_{gg}) \left( \frac{\mu_{ge}^2}{E_{ge}^2} \right) \quad (2)$$

where  $g$  labels the ground state,  $e$  labels the charge-transfer excited state,  $\mu$  is the dipole matrix element between the subscripted states, and  $E$  is the transition energy between the two states. The terms in this equation are proportional to (1) the dipole moment change between the two states, (2) the square of the transition dipole moment between the two states and, (3) the inverse square of the transition energy between the ground and charge-transfer (CT) states. Most molecules that have been explored for NLO applications have dominantly aromatic ground states. The corresponding charge-transfer states have predominantly quinonal ring structures. Electronic polarization, arising from an applied electric field, results in a perturbed ground-state wave function with increased quinonal character and decreased resonance stabilization energy (Figure 1a). Thus, the aromatic ground state impedes electronic polarization in an applied field and effectively reduces the donor and acceptor strengths of a given pair connected by an aromatic bridge.

The visible absorption maximum and extinction coefficients of merocyanines (Figure 1 b and 1 c) are sensitive to the dielectric properties of the surrounding medium. Although solvatochromic behavior is usually

interpreted solely as a change in the electronic distribution at a fixed nuclear geometry (4), for merocyanines it has been shown that the molecular geometry also undergoes significant changes as well (5-11). Thus, in more polar solvents, merocyanines exhibit a change in bond length alternation and a larger ground-state dipole moment ( $\mu$ ). Furthermore, by varying the strength of the donor and acceptor end groups of merocyanine molecules, the ground-state polarization and bond length alternation can also be tuned. Thus, merocyanine molecules are of particular interest as model systems for developing structure/property relationships for NLO.

Many computational studies of molecular hyperpolarizability using either the sum-over-states (SOS) (12) or finite-field (FF) (13) methods employ computed molecular geometries. In these cases, the geometry is explicitly being computed for a molecule in the gas phase. In this environment, charge separation is not stabilized by any solvent-solute interactions and is therefore energetically costly and disfavored. Since the vast majority of molecules that have been explored for their nonlinear optical response have dominantly aromatic ground states which resist charge-transfer polarization (1) they likely exhibit relatively little charge separation, and little change in geometry when comparing their gas phase and solution structures. Thus, for these systems, gas phase computations of geometry and optical properties including hyperpolarizabilities often agree reasonably well with those measured in solution (12, 14). Ignoring the medium dependence of the chemical structure of merocyanines, however, will tend to underestimate the charge-transfer contribution to their ground-state wave

function in most solvents (6) leading to calculated hyperpolarizabilities that can differ significantly with those measured in solution (15).

## Results and Discussion

### *Method*

We sought to develop a computational procedure to vary systematically the ground-state polarization of a molecule and observe the resulting changes in bond length alternation,  $\alpha$ ,  $\beta$ , and  $\gamma$ . Ideally, we would like to be able to accurately describe the geometry and electronic structure of various donor/acceptor molecules in solvent environments of varying polarity and polarizability. Currently, several research groups are developing procedures to simulate the effects of solvent upon polarizable molecules (16, 17). When these techniques have been optimized, it will be of great interest to couple them with computational analyses of hyperpolarizabilities. At this time, one simple way to polarize a molecule is to apply an external electric field and permit the molecule to assume a new equilibrium geometry and electronic configuration. *Although the polarizations in a molecule created by donors and acceptors or by solvent stabilization of charge-separation are not strictly analogous to polarization created by an external electric field, it will be shown that this method qualitatively reproduces experimental trends in geometry and polarizabilities as a function of increasing ground-state polarization.*

Using the AM1 parameterization in the MOPAC software package (18, 19) several prototypical merocyanines (1, 2, 3) and a cyanine (4) were examined

---

under the influence of an external electric field designed to vary the ground-state polarization and geometry. This electric field was defined by two positive and two negative point charges (Sparkles) moved in steps from 40 Å to 4 Å from each end of the molecule as is shown in Figures 2 and 3, The step increment became smaller as the point charges approached the molecule and the change in electric field with a change in distance became larger, beginning with an increment of 10 Å (40 Å, 30 Å, 20 Å), followed by an increment of 1 Å (15 Å through 10 Å) and ending with an increment of 0.2 Å (10 Å through 4 Å). At each fixed Sparkle distance, the geometry was optimized, and  $\mu$ ,  $\alpha$ ,  $\beta$  and  $\gamma$  were calculated by a finite field subroutine (13) in the presence of these point charges. It is important to note that although two explicit fields are applied to the molecule, the external point charge field and the electric field within the finite field calculation, these fields have distinctly different effects on the molecule. In particular, the first field is permitted to influence both its geometric and electronic structure. Thus, at the start of the finite field computation, the molecule is in a new equilibrium geometry and electronic configuration, within which the hyperpolarizabilities are then calculated, By varying the strength of the electric field employed in the finite field routine both numerical accuracy problems and electron configurational changes, observed for field strengths that are too small and large, respectively were avoided. Using external point charges to polarize the electrons without permitting the polarized molecular geometry to change results in a finite field calculation of a molecule in a non-equilibrium geometry. Likewise, removal of the point charges after geometry optimization, but before the finite field procedure leaves nuclei in a position corresponding to a polarized molecule, but removes the external electric field that

stabilizes the polarization. Both of the above procedures were performed; however, for each case, since the nuclei and the electrons were not in equilibrium configurations, much larger external electric fields were needed to polarize the molecule, as compared to applying a field and allowing the geometry to optimize. These results suggested to us that both the applied electric field and the position of the nuclei make important contributions to the polarization response and that the most reasonable procedure was to account for both effects.

As noted earlier, polarization by external point charges is a crude equivalent to that achieved by variation of donor/acceptor strengths. One simple test of the validity of this approximation was to examine the cyanine compounds 4 and 5 where the polarization was varied both by chemical substitution and by using an external point charge. In the first case, asymmetry was induced in the normally symmetric chromophore by sequentially substituting hydrogen atoms upon the methyl groups on one end of the molecule with fluorine atoms. Increases in bond length alternation from the initially bond equivalent, symmetrical cyanine were observed as the number of fluorines in the molecule increased. Likewise, increased bond length alternation was observed as a single, negative point charge was brought closer to the positively charged cyanine as shown in Figure 3. As can be observed in Figure 4, when the hyperpolarizabilities for these two types of asymmetric cyanines were plotted versus bond length alternation, the resulting curves were qualitatively similar. Although the two curves were not superimposable, bond length alternation at the maxima, minima and zero crossings for the two cases were within less than 0.01 Å of each other.



In as much as our goal is to explore the relationship between chemical structure and molecular hyperpolarizabilities, it was encouraging to find that, for this particular case, polarization by an external point charge approximates that induced by chemical substitution.

### *Effect of molecular topology*

Compounds **1** through **3** all contain similar donors and acceptors, but have different topologies, leading to differing degrees of aromaticity for the neutral (non-charge-separated) canonical resonance forms. In the absence of external point charges, the optimized geometries for **1** through **3** exhibit a neutral, bond length alternated structure consistent with what would be expected in the absence of an  $\pi$  stabilization of charge-separation (e.g. structure in the gas phase). In **1** through **3**, the double bonds not part of aromatic rings (e.g., C<sub>2</sub>-C<sub>3</sub> in **1** and **2**, and C<sub>1</sub>-C<sub>2</sub> in **3**, as shown in Figure 2) smoothly change from short ( $\approx 1.36$  Å) to long ( $\approx 1.43$  Å) and the non-ring single bonds (e.g. C<sub>1</sub>-C<sub>2</sub> in **1** and **2**, C<sub>2</sub>-C<sub>3</sub> in **3**, Figure 2) change from long ( $\approx 1.43$  Å) to short ( $\approx 1.36$  Å) as the point charges move closer to the end groups of the molecule. At the same time, the ground-state dipole moment of each molecule increases smoothly. Despite the fact that molecule **1** in the gas phase is calculated to exhibit a neutral, bond alternated structure, there is experimental evidence that, in solution, the molecule is biased towards the zwitterionic structure. For example, **1** exhibits negative solvatochromism (20) (e.g. a blue shift in the optical absorption maximum with increasing solvent polarity) and a negative  $\beta$  (21) consistent with a

larger ground- than excited-state dipole moment (Figure 1b, right). In addition, the three-bond  $^1\text{H}$ - $^1\text{H}$  NMR coupling constant for  $\text{C}_2$ - $\text{C}_3$  of **1** (Figure 2) in polar solvents is roughly 15.5 Hz, indicative of a *trans* carbon-carbon double bond (6). crystal structures of  $(\text{CH}_3)_2\text{N}-(\text{CH}=\text{CH})_3\text{-CHO}$  (6) (11) (average  $r(\text{C}=\text{C}) = 1.356 \text{ \AA}$ ,  $r(\text{C}-\text{C}) = 1.416 \text{ \AA}$  and a difference of  $0.06 \text{ \AA}$ ) and  $(\text{CH}_3)_2\text{N}-(\text{CH}=\text{CH})_3\text{-CHC}(\text{CN})_2$  (7) (11) (average  $r(\text{C}=\text{C}) = 1.376 \text{ \AA}$ ,  $r(\text{C}-\text{C}) = 1.381 \text{ \AA}$ , a difference of less than  $0.01 \text{ \AA}$ ) provide direct evidence for decreased bond length alternation in simple donor-acceptor polyenes relative to unsubstituted polyenes (average  $r(\text{C}=\text{C}) = 1.340 \text{ \AA}$ ,  $r(\text{C}-\text{C}) = 1.445 \text{ \AA}$ , a difference of  $0.11 \text{ \AA}$  from the crystal structure of 1,3,5,7-octatetraene (8) (22) and diphenyl-1,3,5,7-octatetraene (9) (23)) Stilbenes contain aromatic rings that lose aromaticity upon charge separation and are expected to enforce bond length alternation. For example, in the crystal of 2-methoxy-4'-nitro-stilbene (**10**),  $r(\text{C}=\text{C}) = 1.31 \text{ \AA}$ , average  $r(\text{C}-\text{C}) = 1.47 \text{ \AA}$ , and bond length alternation  $A = 0.16 \text{ \AA}$  (24). Using external point charges, **1** through **3** could be polarized into a configuration in which there was no bond length alternation, corresponding to a cyanine-like molecule. At this point, the two limiting resonance forms, displayed for three types of molecules in Figure 1, have approximately the same contribution to both the ground and excited states (25). For **1**, **2** and **3**, zero bond length alternation (see Figure 2) occurred when the external point charges were  $7.6 \text{ \AA}$ ,  $5.6 \text{ \AA}$  and  $4.6 \text{ \AA}$  from the end group heteroatoms (corresponding to an average external electric field along the molecular axis of  $3.5 \times 10^{-3} \text{ au}$ ,  $4.9 \times 10^{-3} \text{ au}$ , and  $6.6 \times 10^{-3} \text{ au}$ . respectively. The

gain in aromaticity upon charge separation in **1** is clearly seen to stabilize the charge-separated form at a given external point charge distance, accounting for this offset. Likewise, the loss in aromaticity upon charge separation in **3** requires a greater electric field to polarize the molecule to this point,

#### *Molecular structure-property relationships*

The basic shapes of the curves for  $\mu$ ,  $a$ ,  $\beta$  and  $\gamma$  versus bond length alternation were the same for the three molecules (Figure 5). Specifically, maxima, minima, and zero crossings occur at roughly the same bond length alternations in each case. Here, the reported dipole is that induced in the molecule (e. g.  $\mu = \mu_{\text{ensemble}} - \mu_{\text{point charge field}}$ ). The peak values of linear and nonlinear polarizabilities of **2** and **3** were greater than those of **1**, most likely because the former two molecules are longer. Our calculations show a peaked  $a$  for **1** through **3** within 0,01 Å of the cyanine limit (zero bond length alternation), consistent with the observation that cyanines are the most polarizable class of linear conjugated organic molecules examined to date (25). At this point, however, large but approximately equal ground- and excited-state dipole moments are expected and  $\beta$ , which is proportional to their difference, is approximately zero, consistent with the predictions of the two-state model (Equation 2). Indeed, the shapes of  $\beta$  curves are consistent with those previously predicted based on a four orbital calculation and observed in the solvent dependent study of  $\beta$  for dimethylindoleaniline (1),

The detailed dependence of  $\gamma$  as a function of ground-state polarization, bond length alternation, and its behavior as compared to  $\alpha$  and  $\beta$  has not been previously described, to our knowledge. There are several important structure/property predictions that result from our analysis. First, the  $\gamma$  curves for all three molecules exhibit negative peaks at zero bond length alternation and positive peaks at either positive or negative bond length alternation. Second, the negative peak values are somewhat larger than the positive peak values. Third, 2, at its positive peak, has a 2- to 4-fold enhancement of  $\gamma$  relative to that of a nonpolarized (unsubstituted) polyene of comparable length ( $\gamma = 5.45 \times 10^{-34}$  esu for 2 vs.  $1.22 \times 10^{-34}$  esu. for a 10 carbon polyene and  $2.47 \times 10^{-34}$  esu for a 12 carbon polyene) (27). Fourth,  $\gamma$  peaks at larger absolute values of bond length alternation than  $\beta$  and in fact when  $\beta$  is peaked,  $\gamma$  is roughly zero. Qualitatively, the behavior of  $\gamma$  predicted here is consistent with that predicted by a three term model previously derived from perturbation theory (28-31) in which:

$$\gamma \propto -\left(\frac{\mu_{ge}^4}{E_{ge}^3}\right) + \left(\frac{\mu_{ge}^2 \mu_{ce}^2}{E_{ge}^2 E_{ge'}}\right) + \left(\frac{\mu_{ge}^2 (\mu_{ce} - \mu_{gg})^2}{E_{ge}^3}\right) \quad (3)$$

where g and e are labels as in the two-state expression above, and e' labels a second excited state. When the first term is dominant, negative  $\gamma$  results which is the case for cyanines (32), and related squarylium dyes (33). For centrosymmetric polyenes, the second term dominates and the third term is zero resulting in positive  $\gamma$  (32, 34). Enhanced  $\gamma$  in donor/acceptor diphenyl

polyenes relative to their centrosymmetric parent compounds has also been observed (26, 35). For these types of polarized polyenes, the third term will enhance  $\gamma$  however, since  $(\mu_{ee}-\mu_{gg})$  exhibits a peak as function of decreasing bond length alternation (1) and goes through zero at roughly zero bond length alternation, its contribution will be small near the cyanine limit. Furthermore, since  $(\mu_{ge}^4/E_{ge}^3)$  also increases with decreasing ground-state bond length alternation (1) and is of opposite sign to the third term, this simple analysis of the perturbation theory expression can explain the peaked  $\gamma$  curves that we predict using MOPAC. Recently,  $\gamma$  values for  $(CH_3)_2N-(CH=CH)_3-CHO$  (6) and  $(CH_3CH_2CH_2CH_2)_2N-(CH=CH)_2-CH=C(CN)_2$  (11) have been measured by third-harmonic generation at 1.907  $\mu m$  in a variety of solvents ranging in polarity from  $CCl_4$  to  $CH_3OH$  (36). The donor-acceptor polyene (6) with a moderately strong formyl acceptor had positive values of  $\gamma$  which exhibit a peak as a function of increasing solvent polarity. In contrast, the related dicyanovinyl compound (11) had positive  $\gamma$  values in nonpolar solvents, but increasingly negative values in solvents of moderate to high polarity. These solvent dependent hyperpolarizabilities were associated with a change from a highly bond length alternated, polyene-like structure for (6) in nonpolar solvents, to a cyanine-like structure with very little bond length alternation for (11) in polar solvents (36). Thus, for these two compounds, the two plots of  $\gamma$  versus solvent polarity are consistent with the predictions of these electric field dependent calculations of hyperpolarizability.

## Conclusions

These external electric field dependent calculations of hyperpolarizabilities allow one to correlate bond length alternation with  $\alpha$ ,  $\beta$  and  $\gamma$ . Furthermore, where experimental and theoretical comparisons are available, there is good qualitative agreement with the results of these calculations, suggesting that this method can be used generally to map out trends in structure/property relationships for different molecular topologies. In addition, the marked sensitivity of  $\alpha$ ,  $\beta$  and  $\gamma$  upon point charge distance (external electric field strength) underscores the need to account for medium dependent changes in both electronic and geometric structure if one is to develop an understanding of structure/property relationships for organic molecules in condensed phases.

By the correct choice of the degree of aromatic-quinonal character in the ground-state wave function it should be possible to strike the optimal compromise for the relative energetic of the neutral and CT resonance forms needed to optimize these quantities. It has been shown that bond length alternation is a key structurally observable parameter that can be correlated with hyperpolarizabilities and is extremely relevant to the optimization of molecules and materials. The  $\beta$  is predicted to peak at  $\approx 0.04 \text{ \AA}$  of bond length alternation. Likewise,  $\gamma$  is predicted to have a positive peak at  $\approx 0.06 \text{ \AA}$  of bond length alternation and a negative peak of larger magnitude at zero bond length alternation. Most molecules currently under investigation have  $\approx 0.10 \text{ \AA}$  or more bond length alternation. This study suggests that such molecules have too much bond length alternation to maximize  $|\beta|$  or  $|\gamma|$ .

### Acknowledgements

We thank Brian Pierce, David Beratan, Steve Risser, Kian-Tat Lim, Bruce Tiemann, Gerald Meredith, and David Dixon for helpful discussions and insights. The work in this paper was performed, in part, at the Center for Space Microelectronics Technology, Jet Propulsion Laboratory (JPL), California Institute of Technology under contract with the National Aeronautics and Space Administration (NASA). The work was sponsored by the Advanced Research Projects Agency through a contract administered by the Air Force Office of Scientific Research and the Ballistic Missile Defense Organization/Innovative Science and Technology Office. Support from the National Science Foundation (Grant CHE-91 06689) and Air Force Office of Scientific Research (Grant F49620-92-J-01 77) is also gratefully acknowledged. CBG thanks the JPL directors office for postdoctoral fellowship.

### References

1. Marder, S. R., Beratan, D. N. & Cheng, L.-T. (1991) Science 252, 103-106.
2. Oudar, J. L. & Chemla, D. S. (1977) J. Chem. Phys. 66, 2664-2668.
3. Lalama, S. J. & Garito, A. F. (1979) Phys. Rev. A 20, 1179,

4. Paley, M. S., Harris, J. M., Looser, H., Baumert, J. C., Bjorklund, G. C., Jundt, D. & Twieg, R. J. (1989) J. Org. Chem. 54,3774-3778.
5. Nolte, K. D. & Dähne, S. (1977) Adv. Mol. Relax. Interact. Proc. 10, 299-329.
6. Benson, H. G. & Murrell, J. N. (1972) J. Chem. Soc., Faraday Trans. II 68, 137-143.
7. Scheibe, P., Schneider, S., Dörr, F. & Daltrozso, E. (1976) Ber. Buns. Ges. 80, 630-638.
8. Radeaglia, R., Engelhardt, G., Lippmaa, E., Pehk, T., Nolte, K. D. & Daehne, S. (1972) Org. Magn. Resonance 4,571 -576.
9. Radeaglia, R. & Dähne, S. (1970) J. Mol. Struct. 5,399-411.
10. Marder, S. R., German, C. B., Cheng, L.-T. & Tiemann, B. G. (1993) Proc. SPIE 1775, 19-31.



11. Marder, S. R., Perry, J. W., Tiemann, B. G., German, C. B., Biddle, S., Gilmour, S. & Bourhill, G. (1993) J. Am. Chem. Soc. 115, 2524-2526.
12. Morley, J. O., Docherty, V. J. & Pugh, D. (1987) J. Chem. Soc., Perkin Trans. II 1351-1355.
13. Kurtz, H. A., Stewart, J. J. P. & Dieter, K. M. (1990) J. Comput. Chem. 11, 82-87.
14. Li, D., Ratner, M. A. & Marks, T. J. (1988) J. Am. Chem. Soc. 110, 1707-1715.
15. Marder, S. R., German, C. B., Tiemann, B. G. & Cheng, L.-T. (1993) J. Am. Chem. Soc. 115, 3006-3007.
16. Luzhkov, V. & Warshel, A. (1991) J. Am. Chem. Soc. 113, 4491-4499.
17. Karelson, M. M. & Zerner, M. C. (1992) J. Phys. Chem. 96, 6949-6957.
18. Stewart, J. J. P. (1989) J. Comput. Chem. 10, 209-220.

19. Stewart, J. J. P. (1989) J. Comput. Chem. 10, 221-264.
20. Brooker, L. G. S., Keyes, G. H. & Heseltine, D. W. (1951) J. Am. Chem. Soc. 73, 5350-5356.
21. Levine, B. F., Bethea, C. G., Wasserman, E. & Leenders, L. (1978) J. Chem. Phys. 68, 5042-5045.
22. Baughman, R. H., Kohler, B. E., Levy, I. J. & Spangler, C. (1985) Synth. Met. 11, 37-52.
23. Drenth, W. & Wiebenga, E. H. (1955) Acts Cry&8, 755-760.
24. Grubbs, R. B., Marder, S. R., Perry, J. W. & Schaefer, W. P. (1991) Chem. Mater. 3, 3-4.
25. Dähne, S. & Nolte, K. D. (1972) J. Chem. Soc., Chem. Commun. 1056-1057.
26. Cheng, L.-T., Tam, W., Marder, S. R., Steigman, A. E., Rikken, G. & Spangler, C. W. (1991) J. Phys. Chem. 95, 10643-10652.

27. Kurtz, H. A. (1990) Int. J. Quant. Chem. Quant. Chem. Symp. 24, 791-798.
  
28. Garito, A. F., Heflin, J. R., Wong, K. Y. & Zamani-Khamiri, O. (1989) in Organic Materials for Non-linear Optics: Royal Society of Chemistry Special Publication No. 69, eds. Harm, R. A. & Bloor, D. (Royal Society of Chemistry, Burlington House, London) pp. 16-27.
  
29. Dirk, C. W. & Kuzyk, M. G. (1991) in Materials for Nonlinear optics: Chemical Perspectives, ACS Symposium Series, eds. Marder, S. R., Sohn, J. E. & Stucky, G. D. (American Chemical Society, Washington, DC), Vol. 455, pp. 687-703.
  
30. Pierce, B. M. (1991) Proc. SPIE 1560, 148-161.
  
31. Kuzyk, M. G. & Dirk, C. W. (1990) Phys. Rev. A 41, 5098-5109.
  
32. Stevenson, S. H., Donald, D. S. & Meredith, G. R. (1988) in Nonlinear Optical Properties of Polymers, Materials Research Society Symposium Proceedings, eds. Heeger, A. J., Orenstein, J. & Ulrich, D. R. (Materials Research Society, Pittsburgh), Vol. 109, pp. 103-108,

33. Dirk, C. W., Cheng, L.-T. & Kuzyk, M. G. (1992) Int. J. Quant. Chem. 43,27-36.
34. Perry, J. W., Steigman, A. E., Marder, S. R., Coulter, D. R., Beratan, D. N., Brinza, D. E., Klavetter, F. L. & Grubbs, R. H. (1988) Proc. SPIE 971, 17-24.
35. Cheng, L.-T., Tam, W., Stevenson, S. H., Meredith, G. R., Rikken, G. & Marder, S. R. (1991) J. Phys. Chem. 95, 10631-10643.
36. Marder, S. R., Perry, J. W., Bourhill, G. H., German, C. B., Tiemann, B. G. & Mansour, K. (1993) Science 261, 186-189.

### Figure Captions

Figure 1. Limiting resonance structures for molecules (a) with an aromatic ground state where resonance energy is lost in the CT state, (b) with a quinonal ground state where resonance energy is gained in the CT state and (c) with a polyene ground state where resonance energy does not change in the CT state.

Figure 2, Molecules 1 through 3 represented in their the neutral (non-charge-separated) resonance structures. The external point charges lie perpendicular to the plane of the molecule at a distance( $r$ ) from the nitrogen and oxygen atoms. Bond length alternation (BLA) is defined so that a large negative value results for the molecule in its neutral form, For **1**,  $BLA = (r(C_1-C_2) + r(C_3-C_4))/2 - r(C_2-C_3)$ . For **2**,  $BLA = (r(C_1-C_2) + r(C_3-C_4) + r(C_5-C_6))/3 - (r(C)-Cl) + r(C_2-C_3) + r(C_4-C_5))/3$ . For **3**,  $BLA = r(C_2-C_3) - (r(C_1-C_2) + r(C_3-C_4))/2$ . In each case,  $r(C_a-C_b)$  is the distance between carbon atoms a and b in Å.

Figure 3. The structures of molecules 4 and 5. For each, bond length alternation is defined as  $BLA = (r(C_2-C_3) + r(C_4-C_5) + r(C_6-C_7))/3 - (r(C_1-C_2) + r(C_3-C_4) + r(C_5-C_6))/3$ . In 4, a single external point charge counterion is brought up to a positively charged, symmetric cyanine. Increases in bond length alternation are calculated and plotted in Figure 4. For 5, increases in bond length alternation are observed as hydrogen atoms

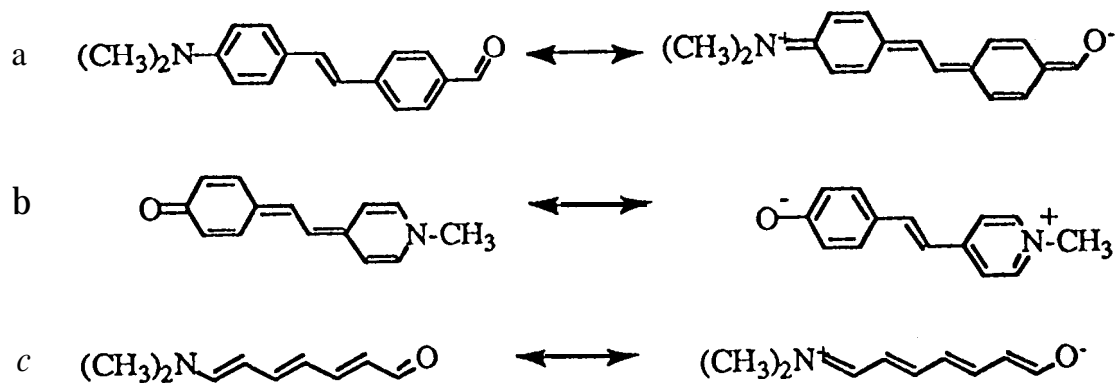
upon the methyl groups at one end of the molecule are **replaced** by fluorine atoms,

Figure 4, [Upper left] Sparkle distance ( $r$ , in Å, as defined in the caption for Figure 3) for 4 and number of fluorines on S; [upper right] linear polarizability ( $\alpha = (\alpha_{xx} + \alpha_{yy} + \alpha_{zz})/3$ ); [lower left] first hyperpolarizability ( $\beta_{xxx}$ ,  $x$  = molecular axis); and [lower right] second hyperpolarizability ( $\gamma = (1/5) \cdot [\gamma_{xxxx} + \gamma_{yyyy} + \gamma_{zzzz} + 2 \cdot (\gamma_{xxyy} + \gamma_{xxzz} + \gamma_{yyzz})]$ ) as a function of bond length alternation (differences between double (D) and single (S) bond lengths as defined in Figure 3) in 4 (circles) and 5 (boxes). Deviations in the  $\beta_{xxx}$  curves between 4 and 5 result partially from slight differences in the orientation of the molecular axis with respect to the x-axis.

Figure 5. [Upper left] Sparkle distance ( $r$ , in Å as defined in the caption for Figure 2, open symbols) and computed dipole moment ( $p$ , filled symbols); [upper right]  $\alpha$ ; [lower left]  $\beta$ ; and [lower right]  $\gamma$  as a function of bond length alternation (as defined in Figure 2) in 1 (boxes) and 2 (circles) and 3 (triangles).

German and Marder, An Investigation of the Interrelationships...

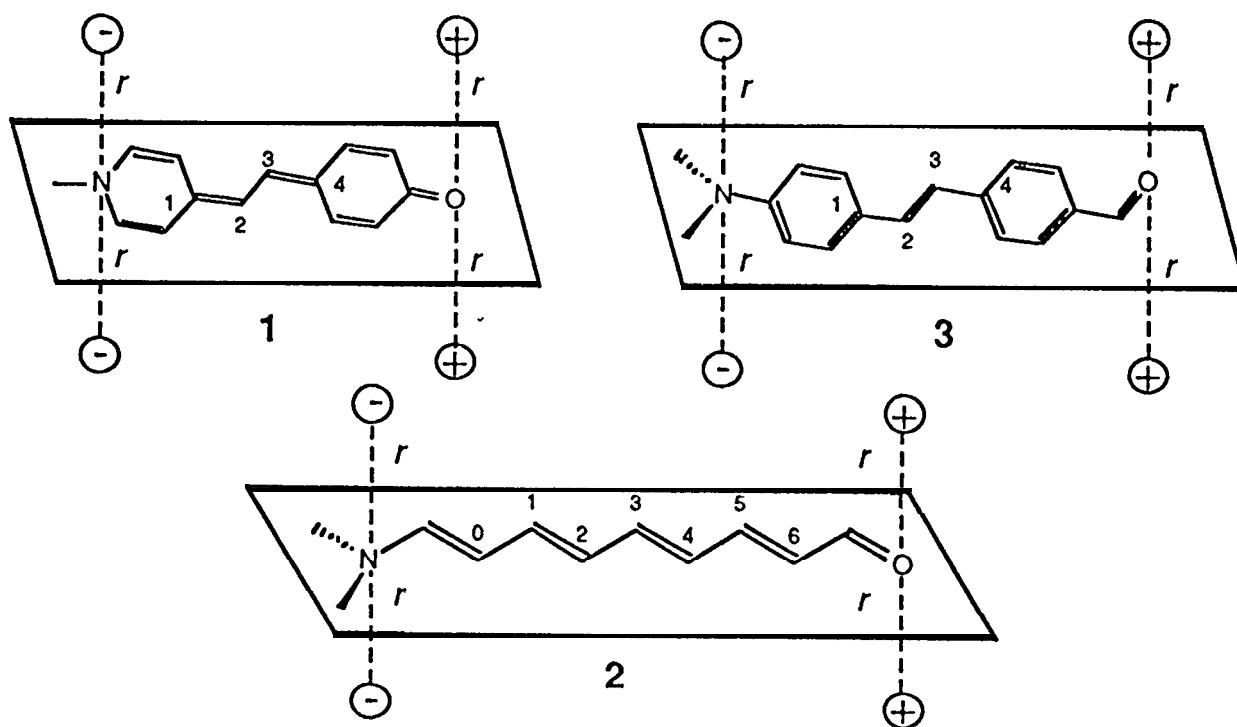
Figure 1



Sized for reduction to 53% of present size.  
 Reduced figure without legend occupies 0.27 page.  
 Reduced figure occupies 2 column width space.

Figure 2

PNAS No. # V0904 Fig. 2  
Reduce to \_\_\_\_\_ % of original

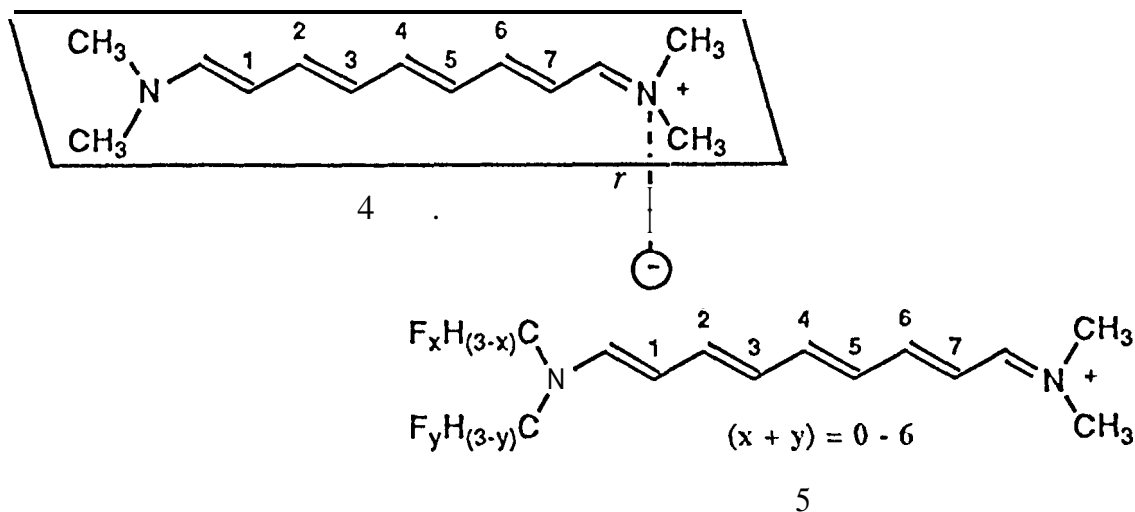


Sized for reduction to 50 % of present size.  
Reduced figure without legend occupies 2.11 page.  
Reduced figure occupies 1 2 column width space.



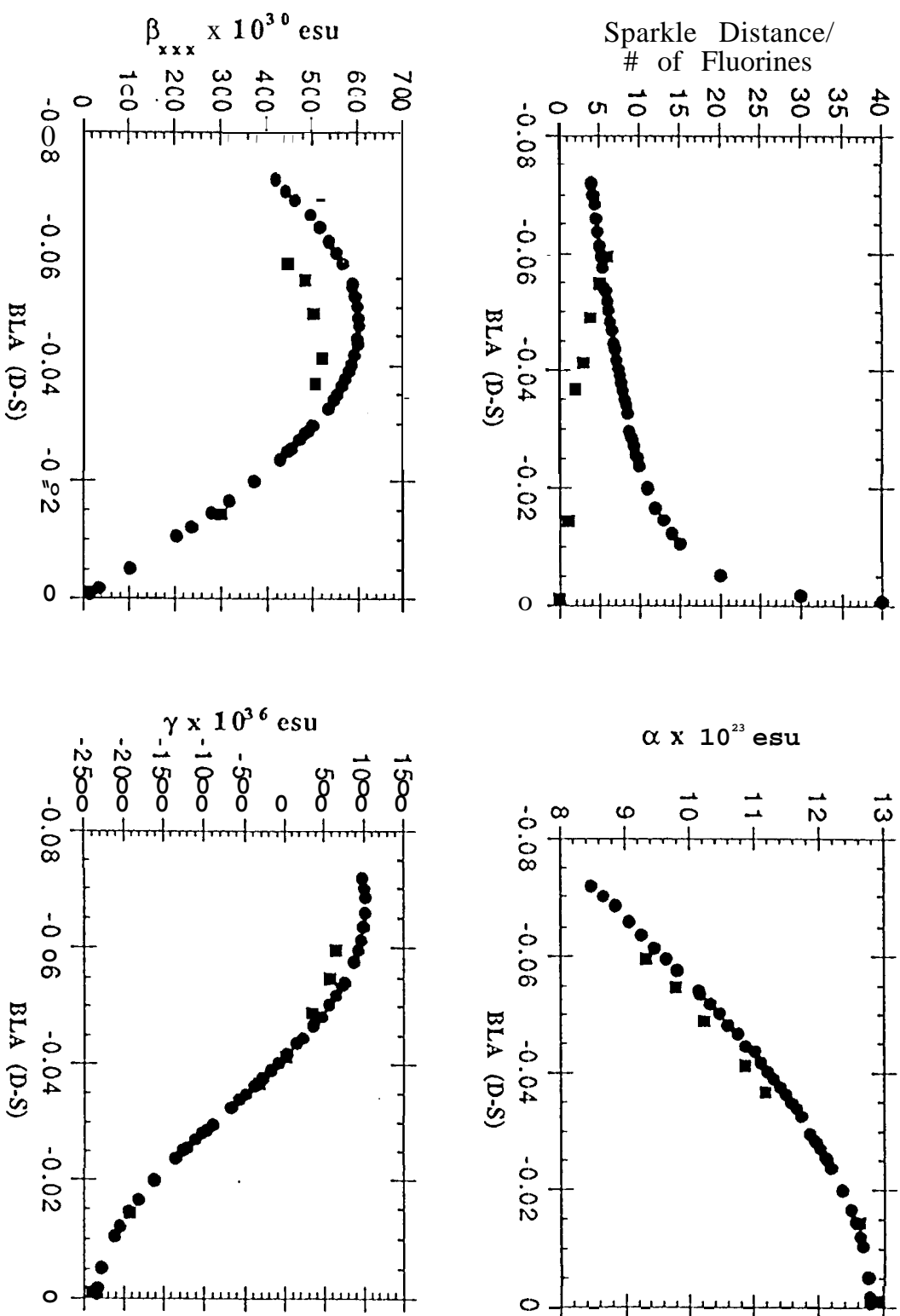
"Gorman and Marder, An Investigation of the Interrelationships...

Figure 3



Sized for reduction to 51 % of present size.  
 Reduced figure without legend occupies 2.21 page.  
 Reduced figure occupies 92 column width space.

Figure 4



Sized for reduction to 57% of present size.  
 Reduced figure without legend occupies 1/4 page.  
 Reduced figure occupies 1/2 column width space.

Figure 5

